



**HAL**  
open science

## **In-situ forming plga implants for intraocular dexamethasone delivery**

C. Bode, Heiko Kranz, Florence Siepmann, Juergen Siepmann

► **To cite this version:**

C. Bode, Heiko Kranz, Florence Siepmann, Juergen Siepmann. In-situ forming plga implants for intraocular dexamethasone delivery. *International Journal of Pharmaceutics*, 2018, *International Journal of Pharmaceutics*, 548, pp.337-348. 10.1016/j.ijpharm.2018.07.013 . hal-04467257

**HAL Id: hal-04467257**

**<https://hal.univ-lille.fr/hal-04467257v1>**

Submitted on 29 Apr 2024

**HAL** is a multi-disciplinary open access archive for the deposit and dissemination of scientific research documents, whether they are published or not. The documents may come from teaching and research institutions in France or abroad, or from public or private research centers.

L'archive ouverte pluridisciplinaire **HAL**, est destinée au dépôt et à la diffusion de documents scientifiques de niveau recherche, publiés ou non, émanant des établissements d'enseignement et de recherche français ou étrangers, des laboratoires publics ou privés.

1  
2  
3  
4  
5  
6  
7  
8  
9  
10  
11  
12  
13  
14  
15  
16  
17  
18  
19  
20  
21  
22  
23  
24  
25

Research article

***In-situ* forming PLGA implants for intraocular dexamethasone delivery**

C. Bode,<sup>1</sup> H. Kranz,<sup>2</sup> F. Siepmann,<sup>1</sup> J. Siepmann,<sup>1,\*</sup>

<sup>1</sup>*Univ. Lille, Inserm, CHU Lille, U1008, 59000 Lille, France*

<sup>2</sup>*Bayer AG, Muellerstraße 178, 13353 Berlin, Germany*

\*correspondence:

Professor Juergen Siepmann, Ph.D.

Univ. Lille, College of Pharmacy,

INSERM U1008 Controlled Drug Delivery Systems and Biomaterials

3, rue du Professeur Laguesse

59006 Lille, France

Phone: +33-3-20964708

juergen.siepmann@univ-lille2.fr

26 **Abstract**

27 Different types of *in-situ* forming implants based on poly(lactic-co-glycolic acid) (PLGA) and  
28 N-methyl-pyrrolidone (NMP) were prepared for controlled ocular delivery of dexamethasone.  
29 The impact of the volume of the release medium, initial drug content, polymer molecular weight  
30 and PLGA concentration on the resulting drug release kinetics were studied and explained  
31 based on a thorough physico-chemical characterization of the systems. This included for  
32 instance the monitoring of dynamic changes in the implants' wet and dry mass, morphology,  
33 PLGA polymer molecular weight, pH of the surrounding bulk fluid and water/NMP contents  
34 upon exposure to phosphate buffer pH 7.4. Importantly, the systems can be expected to be rather  
35 robust with respect to variations in the vitreous humor volumes encountered *in vivo*.  
36 Interestingly, limited drug solubility effects *within* the implants as well as in the surrounding  
37 aqueous medium play an important role for the control of drug release at a drug loading of only  
38 7.5 %. Furthermore, the polymer molecular weight and PLGA concentration in the liquid  
39 formulations are decisive for *how* the polymer precipitates during solvent exchange and for the  
40 swelling behavior of the systems. These features determine the resulting inner system structure  
41 and the conditions for mass transport. Consequently, they affect the degradation and drug  
42 release of the *in-situ* formed implants.

43

44 *Key words:* PLGA; *in-situ* forming implant; dexamethasone; autocatalysis; swelling

## 45 1. Introduction

46 Age-related macular degeneration (AMD) and diabetic retinopathy are two of the leading  
47 causes for irreversible blindness and vision impairment (Hughes et al., 2005; Edelhauser et al.,  
48 2010). Late AMD exists in two forms: the atrophic (or “dry”) AMD and the neovascular (or  
49 “wet”) AMD. Yet, up to now, wet AMD is the only treatable form. It is triggered by vascular  
50 endothelial growth factor (VEGF), causing the blood vessels in the retina to grow erratically,  
51 eventually breaking through the Bruch’s membrane (the innermost layer of the choroid). This  
52 leads to blood and protein leakage in the macula, resulting in a blurry vision or sudden vision  
53 loss (Chiou, 2011; Bonilha et al., 2013). In the case of diabetic retinopathy, microvascular  
54 complications are the result of poorly adjusted diabetes. Sustained hyperglycaemia ultimately  
55 causes microaneurysms and a breakdown of endothelial tight junctions in the blood-retinal  
56 barrier (BRB), allowing proteins to leak into the vitreous. At later stages, choroidal  
57 neovascularization of the retina occurs (Kowluru and Mishra, 2015; Wan et al., 2015; Zaki et  
58 al., 2016). Both diseases (wet AMD and diabetic retinopathy) are commonly treated by  
59 intravitreal injections of anti-VEGF agents and corticosteroids. Anti-VEGF agents inhibit the  
60 growth of the blood vessels, while corticosteroids reduce inflammation by minimizing the  
61 expression of inflammatory cytokines and of VEGF. Hence, the choroidal neovascularization  
62 is stabilized, decreasing the breakdown rate of the blood-retinal barrier (Kurz et al., 2008;  
63 Wykoff et al., 2015; Rodríguez Villanueva et al., 2017).

64 For an effective treatment, the drugs have to reach the retina in the back of the eye.  
65 However, the anatomy and physiology of the eye hamper this: For instance, when using eye  
66 drops, less than 5% of the administered drug is generally absorbed through the cornea to reach  
67 the anterior chamber (Urtti, 2006). This is due to the low permeability of the cornea (with its  
68 different layers and polarities), dilution with tear fluid, rapid lacrimal drainage and other factors.  
69 Most importantly, only a very small fraction of the drug is finally found inside the vitreous: the

70 site of action (approximately 0.001 – 0.0004 % of the administered drug) (Urtti, 2006; Wilson  
71 et al., 2011; Kaur and Kakkar, 2014). It has to be pointed out that systemic drug administration  
72 also encounters a crucial hurdle: The blood-retinal barrier, preventing most drugs from reaching  
73 the vitreous. The attempt to overcome this hurdle with very high systemically administered  
74 drug amounts to achieve therapeutic levels in the eye is limited by severe side effects  
75 (Edelhauser et al., 2010; Kaur and Kakkar, 2014).

76 For these reasons intravitreal drug injections are currently considered as the most  
77 appropriate way to assure that the drug reaches its site of action. However, every injection bears  
78 a risk of infections and other serious side effects, like retinal detachment, retinal haemorrhage,  
79 endophthalmitis, increased intraocular pressure, cataract or vitreous haemorrhage (Edelhauser  
80 et al., 2010; Giudice and Galan, 2012; Ying et al., 2013; Kaur and Kakkar, 2014; Bisht et al.,  
81 2017). Apart from these risks, the discomfort of receiving a needle in the eye leads to limited  
82 compliance (Droege et al., 2013; Ghazala et al., 2013).

83 To assure treatment efficacy, therapeutic drug concentrations must be provided over  
84 prolonged periods of time at the site of action. Since dexamethasone has a half-life of  
85 approximately 5.5 h in the vitreous, frequent injections are, thus, necessary to remain within  
86 the therapeutic range (Chan et al., 2011). Local controlled drug delivery systems can help  
87 overcoming all these hurdles: The risk of side effects can be reduced, patient compliance  
88 improved and the therapeutic efficacy increased. Nowadays, non-biodegradable implants are  
89 approved by the FDA for intraocular administration, releasing dexamethasone over prolonged  
90 periods of time [e.g., Retisert ([retisert.com](http://retisert.com)), Iluvien ([iluvien.com](http://iluvien.com))]. However, these implants  
91 have to be removed surgically upon drug exhaust, which is associated with similar risks as the  
92 initial insertion, or remain in the vitreous where they accumulate over time (Yasin et al., 2014).  
93 To avoid the second surgery for device removal, *biodegradable* implants offer an interesting  
94 potential. For example, Allergan developed Ozurdex, a biodegradable implant containing 0.7

95 mg dexamethasone in a poly(lactic-co-glycolic acid) (PLGA) matrix, which is injected through  
96 a 22G needle (Chan et al., 2011). But large needles can be problematic in practice. The injection  
97 of a *liquid* solution, that precipitates *in-situ* in the eye and sustains drug release, could  
98 effectively reduce the required needle size. Importantly, smaller needles are associated with  
99 less pain experienced by the patients (Rodrigues et al., 2011).

100 Different types of *in-situ* forming implants have been described in the literature, for various  
101 types of applications (Kranz and Bodmeier, 2007, 2008; Schoenhammer et al., 2009, 2010;  
102 Kempe and Mäder, 2012; Parent et al., 2013, 2017). The transformation from the liquid state  
103 (allowing for facilitated administration) to the solid state (allowing for controlled drug release  
104 over prolonged periods of time) can be induced by different phenomena, such as solvent  
105 exchange, changes in the pH or temperature, or *in-situ* cross-linking (Kempe and Mäder, 2012).  
106 In the case of solvent exchange, generally a water-insoluble polymeric matrix former is  
107 dissolved in a biocompatible, water-miscible organic solvent. The drug is dissolved and/or  
108 dispersed in this polymer solution. Upon injection into aqueous body fluids, the organic solvent  
109 diffuses into the surrounding environment (being miscible with water), while water diffuses  
110 into the formulation. Since the polymer is water-insoluble, it precipitates and forms the solid  
111 implant. The drug molecules or particles are trapped within the implant and slowly released  
112 over time. Different formulation parameters can be used to alter implant formation and  
113 performance. For instance, the addition of hydrophilic polymers [such as hydroxypropyl  
114 methylcellulose (HPMC)] has been proposed to increase the bioadhesion of *in-situ* forming  
115 implants releasing antimicrobial drugs in periodontal pockets for the treatment of periodontitis  
116 (Do et al., 2014, 2015b, 2015a; Agossa et al., 2017). Poly(lactic-co-glycolic acid) (PLGA) is a  
117 well-known biodegradable and biocompatible matrix former in parenteral controlled release  
118 formulations (Kranz et al., 2000; Luan et al., 2006; Desai et al., 2008; Kempe et al., 2010;  
119 Fredenberg et al., 2011; Ghalanbor et al., 2013; Schwendeman et al., 2014; Gasmi et al., 2015a,

120 2015b; Huang et al., 2015; Gasmi et al., 2016; Hirota et al., 2016; Hamoudi-Ben Yelles et al.,  
121 2017). In the case of *in-situ* forming implants based on PLGA, often N-methyl-pyrrolidone  
122 (NMP) is used as a water-miscible organic solvent, for example in the following commercially  
123 available drug products: Atridox (for injection into periodontal pockets) (Thakur et al., 2014);  
124 Eligard (for subcutaneous injection) (eligard.com); Nuflor (for intramuscular or subcutaneous  
125 injection in beef) (merck-animal-health-usa.com/product/cattle/Nuflor-Injectable-Solution/1);  
126 Doxirobe gel (for injection into periodontal pockets in dogs)  
127 (zoetisus.com/products/dogs/doxirobe-gel.aspx). Furthermore, the group of AG Mikos (Ueda  
128 et al., 2007) reported on NMP-based *in-situ* forming ocular drug delivery systems for  
129 luocinolone acetonide, which are based on poly(propylene fumarate) as polymeric matrix  
130 former. It has to be pointed out that the toxicity of NMP upon intraocular injection should be  
131 investigated in the future.

132 The aim of this study was to prepare different types of *in-situ* forming implants based on  
133 PLGA for intraocular dexamethasone delivery. The systems were thoroughly characterized  
134 physico-chemically, including for instance dynamic changes in the wet mass, dry mass,  
135 water/NMP content, morphology, polymer molecular weight, potential changes in the pH of the  
136 release medium, and drug release kinetics.

137

138

## 139 **2. Materials and methods**

140

### 141 **2.1. Materials**

142 Poly(D,L-lactic-co-glycolic acid) (50:50, -COOH end groups; PLGA, Resomer RG 502 H  
143 and Resomer RG 504 H; Evonik, Darmstadt, Germany); dexamethasone (Discovery Fine  
144 Chemicals, Dorset, UK); N-methyl-pyrrolidone, acetonitrile and tetrahydrofuran (Fisher  
145 Scientific, Illkirch, France); ethanol 96% (VWR, Fontenay-sous-Bois, France).

146

## 147 **2.2. Preparation of the liquid formulations**

148 Appropriate amounts of PLGA and dexamethasone were dissolved in NMP in glass vials  
149 under stirring at 500 rpm (Multipoint Stirrer, Thermo Scientific, Loughborough, UK) at room  
150 temperature for 60 min. Afterwards, the vials were kept without stirring for 1 h at room  
151 temperature in order to remove air bubbles. The formulations were stored at 2-8 °C, and allowed  
152 to reach room temperature prior to use.

153

## 154 **2.3. *In-situ* formation of implants**

155 Eppendorf vials were filled with 2.25 or 4.5 mL phosphate buffer pH 7.4 (USP 40) and kept  
156 at 37 °C overnight. One hundred µl of the liquid PLGA/dexamethasone/NMP formulations  
157 (prepared as described in *section 2.2.*) were injected into the vials using a syringe pump  
158 (2 mL/min; PHD 2000; Harvard Apparatus, Holliston, USA). Solvent exchange initiated  
159 polymer precipitation and *in-situ* implant formation. The Eppendorf vials were placed into a  
160 horizontal shaker (80 rpm, 37 °C; GFL 3033, Gesellschaft fuer Labortechnik, Burgwedel,  
161 Germany).

162

## 163 **2.4. Characterization of *in-situ* formed implants**

164 In vitro drug release: At determined time points, the phosphate buffer pH 7.4 was  
165 completely renewed. The amount of dexamethasone in the withdrawn bulk fluid was  
166 determined by HPLC-UV analysis, using a Thermo Fisher Scientific Ultimate 3000 Series  
167 HPLC, equipped with a LPG 3400 SD/RS pump, an auto sampler (WPS-3000 SL) and a UV-  
168 Vis detector (VWD-3400RS) (Thermo Fisher Scientific, Waltham, USA). Samples were  
169 centrifuged for 2.5 min at 10,000 rpm (Centrifuge Universal 320; Hettich, Tuttlingen,  
170 Germany), and filtered with a 0.45 µm PVDF syringe filter (Millex-HV, Merck Millipore,



171 Tullagreen, Ireland). Fifty  $\mu\text{L}$  samples were injected into an A C18 RP column (Gemini 3  $\mu\text{m}$   
 172 C18 110 Å, 100 mm x 4.6 mm; Phenomenex, Le Pecq, France). The mobile phase consisted of  
 173 acetonitrile and water (33:67 v/v), the flow rate was 1.5 mL/min. Dexamethasone had a  
 174 retention time of approximately 3.8 min, the detection wavelength was  $\lambda = 254$  nm. The  
 175 calibration curve was linear ( $R > 0.999$ ) within the range of 0.06 to 0.00003 mg/mL. To  
 176 determine the amount of dexamethasone potentially remaining in the implants after 35 d  
 177 exposure to phosphate buffer pH 7.4, the remnants were freeze-dried for 3 d (Christ Epsilon 2–  
 178 4 LSC; Martin Christ, Osterode, Germany) and the lyophilisates were dissolved in a mixture of  
 179 acetonitrile and ethanol (2:1 v/v). The solutions were filtered using 0.45  $\mu\text{m}$  PVDF filter  
 180 syringes, and analyzed for their drug contents by HPLC-UV (as described above). In case of  
 181 incomplete drug release at the end of the observation period, the “missing” amounts were  
 182 experimentally recovered in the implant remnants. All experiments were conducted in triplicate.  
 183 In addition, the pH of the release medium was measured at pre-determined time points using a  
 184 pH meter (InoLab pH Level 1; WTW, Weilheim, Germany) ( $n = 3$ ).

185 Implant swelling and erosion: At pre-determined time points, implant samples were  
 186 withdrawn, excess water carefully removed using Kimtech precision wipes (Kimberly-Clark,  
 187 Rouen, France) and weighed [*wet mass* ( $t$ )]. The samples were lyophilized for 3 d (Christ  
 188 Epsilon 2–4 LSC) and weighed again [*dry mass* ( $t$ )]. The *wet mass* (%) ( $t$ ), *water/NMP content*  
 189 (%) ( $t$ ), and *dry mass loss* (%) ( $t$ ) were calculated as follows:

$$190$$

$$191 \quad \text{wet mass (\%)(}t\text{)} = \frac{\text{wet mass (}t\text{)}}{\text{formulation mass}} \times 100 \% \quad (1)$$

$$192$$

$$193 \quad \text{water/NMP content (\%)(}t\text{)} = \frac{\text{wet mass (}t\text{)} - \text{dry mass (}t\text{)}}{\text{wet mass (}t\text{)}} \times 100 \% \quad (2)$$

$$194$$

$$195 \quad \text{dry mass loss (\%)(}t\text{)} = \frac{\text{dry mass (0)} - \text{dry mass (}t\text{)}}{\text{dry mass (0)}} \times 100 \% \quad (3)$$

196

197 where *formulation mass* is the initial total mass of the liquid formulation (PLGA +  
198 dexamethasone + NMP), and *dry mass (0)* is the dry mass of the liquid formulation prior to  
199 exposure to the release medium (PLGA + dexamethasone). All experiments were conducted in  
200 triplicate.

201 Polymer degradation: At pre-determined time points, implants were withdrawn, freeze-  
202 dried and the lyophilisates were dissolved in tetrahydrofuran (at a concentration of 3 mg/mL).  
203 The average polymer molecular weight (Mw) of the PLGA was determined by Gel Permeation  
204 Chromatography (GPC, Separation Modules e2695 and e2695D, 2419 RI Detector, Empower  
205 GPC software; Waters, Guyancourt, France) using a PLGel 5  $\mu\text{m}$  MIXED-D column, 7.5 x  
206 300 mm (Agilent Technologies, Interchim, Montluçon, France). The injection volume was  
207 50  $\mu\text{L}$ . Tetrahydrofuran was the mobile phase (flow rate: 1 mL/min). Polystyrene standards  
208 with molecular weights between 1,090 and 70,950 Da (Polymer Laboratories, Varian, Les Ulis,  
209 France) were used to prepare the calibration curve. All experiments were conducted in  
210 triplicate.

211 Implant morphology: At pre-determined time points, implants were withdrawn and  
212 optionally freeze-dried. Cross-sections were obtained by manual breaking. Pictures were taken  
213 with an optical image analysis system (Nikon SMZ-U; Nikon, Tokyo, Japan), equipped with a  
214 Zeiss camera (AxioCam ICc1; Zeiss, Jena, Germany).

215

## 216 **2.5. Determination of the drug solubility**

217 The solubility of dexamethasone (as received) in phosphate buffer pH 7.4 at 37 °C was  
218 determined in agitated glass flasks. An excess amount of dexamethasone powder  
219 (approximately 30 mg) was exposed to 80 mL bulk fluid, kept at 37 °C under horizontal shaking  
220 (80 rpm; GFL 3033). Samples were withdrawn, filtered (0.45  $\mu\text{m}$  PVDF syringe filter), diluted

221 and analyzed for their drug content by HPLC-UV (as described above, using an injection  
222 volume of 20  $\mu$ L) until equilibrium was reached. Each experiment was conducted in triplicate.

223

224

### 225 **3. Results and Discussion**

226

#### 227 **3.1. Importance of the volume of the release medium**

228 Since the investigated implants are formed *in-situ* following solvent exchange, it was  
229 important to evaluate the impact of the volume of the release medium into which the  
230 PLGA/drug/NMP solutions were injected. Potentially, the volume of this aqueous phase can  
231 affect the diffusion rate of NMP into the surrounding aqueous phase and/or the diffusion rate  
232 of water into the (initially) liquid formulation. Such changes might affect the resulting implant  
233 size and inner structure and, hence, the drug release kinetics.

234 The volume of vitreous humor in humans has been reported to be about 4 to 5 mL (Bennett,  
235 2016). To monitor potential effects of variations in the bulk fluid volume in this order of  
236 magnitude on the key properties of the *in-situ* formed implants, 2.25 and 4.5 mL have been  
237 investigated in this study. Furthermore, most drugs are eliminated via the anterior pathway  
238 (Toris et al., 1999; Urtti, 2006). To simulate drug elimination and fluid renewal, the release  
239 medium was completely exchanged every day during the first week (which is most decisive for  
240 implant formation) in this study.

241 Figure 1 shows macroscopic pictures of PLGA-based implants formed upon injection of  
242 100  $\mu$ L of a PLGA/dexamethasone/NMP solution into 2.25 or 4.5 mL phosphate buffer pH 7.4  
243 (37 °C). The liquid formulations contained 30 % Resomer RG 502H and 0.75 %  
244 dexamethasone. The photos were taken after 3 d. At the top, implants in Eppendorf tubes (filled  
245 with the release medium) are shown. Below, higher magnifications of implants, which had been

246 carefully withdrawn from the release medium are illustrated (surfaces). At the bottom, surfaces  
247 and cross-sections of implant samples after freeze-drying are shown. The cross-sections were  
248 obtained by manual breaking. The dashed regions highlight the hollow cores of the implants.  
249 As it can be seen, there was no remarkable impact of the volume of the aqueous bulk fluid (2.25  
250 vs. 4.5 mL) on the resulting implant morphology: left vs. right hand side in Figure 1. Please  
251 note that caution must be paid when drawing conclusions from the pictures of lyophilized  
252 implants, because of artifact creation during freeze-drying. Importantly, the implants were  
253 hollow also in the wet state (data not shown). This can be explained as follows: Upon contact  
254 with water, NMP diffuses into the outer bulk fluid and water diffuses into the liquid NMP  
255 formulation. Since PLGA is soluble in NMP, but not in water, at a certain time point the  
256 polymer precipitates (once the solubility of the polymer in the water/NMP mixture is reached).  
257 This process likely starts at the “formulation – aqueous bulk fluid” interface, because the water  
258 concentration is highest and the NMP concentration lowest at this location. The continuous  
259 decrease in PLGA solubility in the NMP/water mixture (the NMP content decreases, whereas  
260 the water content increases) leads to continued polymer precipitation. Thus, the PLGA “shell”  
261 becomes thicker and thicker, growing “inwards”. Once all PLGA has precipitated, potentially  
262 remaining inner volumes (here the centers of the implants) cannot be filled with polymer and  
263 become water-filled cavities. Please note that complete solvent exchange took up to several  
264 days in this study: Thus, the implant cores remained liquid for a significant period of time.  
265 Importantly, no noteworthy impact of the bulk fluid volume on this cavity formation was  
266 observed.

267 Figures 2a and b show the resulting dexamethasone release kinetics and the dynamic  
268 changes of the systems’ water/NMP contents over time. The water/NMP contents of the  
269 implants were determined gravimetrically as the difference between the wet and dry mass of  
270 the withdrawn samples (before and after freeze-drying). As it can be seen, the drug release

271 curves were virtually overlapping for the investigated bulk fluid volumes (2.25 vs. 4.5 mL).  
272 Also, the resulting water/NMP contents were very similar. This can probably be attributed to  
273 the fact that NMP and water are freely miscible: So, there are no saturation effects, resulting in  
274 potentially reduced NMP diffusion rates into smaller (eventually more saturated) outer aqueous  
275 phases (and vice versa).

276 Importantly, limited drug solubility effects in the surrounding release medium are unlikely  
277 to affect dexamethasone release from the *in-situ* forming implants at an initial drug loading of  
278 0.75 %: The solubility of dexamethasone in phosphate buffer pH 7.4 at 37 °C was determined  
279 to be  $77 \pm 4$  µg/mL. In NMP, the drug is freely soluble. Thus, at early time points (when the  
280 surrounding bulk fluid contains considerable amounts of NMP) saturation effects in the  
281 surrounding bulk fluid are unlikely. Furthermore, even if assuming the absence of any NMP in  
282 the surrounding bulk fluid from day 3 on (this is a “worst case scenario” for the drug solubility),  
283 sink conditions were also provided for the remaining observation period (considering the drug  
284 solubility determined in pure phosphate buffer pH 7.4 at 37 °C).

285 These findings are important, since they demonstrate that variations in the volume of the  
286 bulk fluid into which the PLGA/drug/NMP solutions are injected, are not substantially affecting  
287 the key properties of the resulting implants. In other words: The proposed *in-situ* forming  
288 implant formulations can be expected to be rather robust with respect to variations in the  
289 vitreous humor volumes encountered *in vivo*.

290

### 291 **3.2. Impact of the drug loading**

292 Figure 3 shows the impact of the initial drug loading of the *in-situ* forming implant  
293 formulations on the resulting dexamethasone release kinetics and the dynamic changes in the  
294 implants' wet mass as well as water/NMP contents. The initial drug content was varied from  
295 0.25 to 7.5 %, as indicated. Please note that 100 µL of the formulation with the intermediate

296 drug loading (0.75 %) contain a similar drug dose as the commercially available drug product  
297 Ozurdex (0.7 mg) (Chan et al., 2011). The release medium was 2.25 mL phosphate buffer  
298 pH 7.4. Resomer RG 502H (30 %) was the polymer. Clearly, the relative drug release rates  
299 were similar for formulations loaded with 0.25 and 0.75 % dexamethasone (filled and open  
300 circles in Figure 2a), whereas the relative drug release rate was substantially lower at 7.5 %  
301 drug loading (filled triangles). This cannot be attributed to differences in the dynamic changes  
302 in the systems' wet mass, as illustrated in Figure 3b (which were rather similar for all drug  
303 loadings).

304 Given the limited solubility of dexamethasone in the release medium ( $77 \pm 4 \mu\text{g/mL}$  in  
305 phosphate buffer pH 7.4 at  $37^\circ\text{C}$ ), one hypothesis can be that the substantially reduced drug  
306 release rate at 7.5 % initial dexamethasone loading is due to saturation effects. To evaluate the  
307 validity of this hypothesis, the renewal rate of the release medium was altered: Figures 4a and  
308 b show the resulting drug release kinetics and degrees of bulk fluid saturation (with respect to  
309 the drug) observed at a higher and lower sampling frequency (at each sampling time point, the  
310 release medium was completely renewed). The degrees of saturation of the release medium  
311 were calculated based on the solubility of dexamethasone in phosphate buffer pH 7.4 at  $37^\circ\text{C}$ .  
312 Since the surrounding bulk fluid contained important amounts of NMP at early time points, and  
313 since dexamethasone is soluble in NMP, no values are indicated in the first week (Figure 4b).  
314 Clearly, the higher sampling frequency lead to faster drug release after about 1 week,  
315 corresponding to lower degrees of bulk fluid saturation with the drug. Furthermore, after about  
316 3 weeks, the degree of bulk fluid saturation substantially decreased (to about 10 % = sink  
317 conditions) in the case of the higher sampling frequency, while the release rate *decreased*. These  
318 observations indicate that saturation effects likely refer to both: dexamethasone saturation in  
319 the *surrounding* bulk fluid as well as drug saturation effects *within* the implants: At an initial  
320 drug loading of 7.5 %, important parts of the dexamethasone can be expected to precipitate

321 *within* the *in-situ* forming PLGA implants upon water penetration into and NMP leaching out  
322 of the system. Consequently, dissolved and non-dissolved dexamethasone co-exist within the  
323 implant. It has to be pointed out that only dissolved drug is available for diffusion and can be  
324 released into the surrounding bulk fluid (Siepmann and Siepmann, 2012, 2008). Hence, drug  
325 release is also likely to be limited by saturation effects *within* the implants.

326 Please note that during the first week, the observed dexamethasone release rates were very  
327 similar for the lower and higher sampling frequency (filled and open circles in Figure 4a). This  
328 might be explained by the fact that during this time period noteworthy amounts of NMP were  
329 still present *within* the implants and the surrounding bulk fluid (limiting the importance of drug  
330 saturation effects).

331 Furthermore, the initial drug loading had no major impact on the resulting dynamic changes  
332 in the implants' wet mass over time (Figure 3b). The latter increased during the first 2.5 weeks,  
333 and then decreased again. The initial increase can be attributed to the progressing PLGA  
334 degradation and subsequent water penetration into the more and more hydrophilic polymer  
335 matrices. The subsequent decrease is likely attributable to the dissolution/disappearance of the  
336 remnants (more hydrated regions dissolving faster than less hydrated regions). The water/NMP  
337 contents were very high during the observation period, irrespective of the initial drug loading  
338 (Figure 3c).

339

### 340 **3.3. Impact of the PLGA polymer molecular weight**

341 The effects of the polymer molecular weight of the PLGA on drug release and the dynamic  
342 changes in the implants' wet mass as well as water/NMP contents upon exposure to phosphate  
343 buffer pH 7.4 are illustrated in Figure 5: Resomer RG 502H (Mw about 15 k Da) and Resomer  
344 RG 504H (Mw about 45 k Da) are compared. The initial dexamethasone loading was 0.25 %,   
345 the polymer concentration in the liquid formulation was 30 %, and the volume of the release

346 medium was 2.25 mL. As it can be seen, the polymer molecular weight substantially impacted  
347 the dynamic changes in the systems' wet mass and water/NMP content: Implants based on  
348 longer chain PLGA took up fundamentally less water than systems based on shorter chain  
349 PLGA. This can be attributed to the facts that: (i) longer chain PLGA is more hydrophobic than  
350 shorter chain PLGA, and (ii) longer chain PLGA is likely to precipitate earlier than shorter  
351 chain PLGA upon water penetration into the system and NMP diffusion out of the formulation.  
352 The observed differences in the wet mass of the implants based on shorter and longer chain  
353 PLGA (Figure 5b) are consistent with the different water/NMP contents of systems (Figure 5c).  
354 Whereas the implants based on the more hydrophilic Resomer RG 502H show high water  
355 contents right from the beginning, the water contents of Resomer RG 504H-based systems was  
356 initially substantially lower, but significantly increased during the observation period (due to  
357 the progressive polymer chain cleavage). From a practical point of view, substantial implant  
358 swelling should be avoided to minimize any related side effects in vivo. This might for instance  
359 be achieved via the selection of appropriate PLGA molecular weights or monomer (lactic acid:  
360 glycolic acid) ratios, or specific additives (Do et al., 2014, 2015a,b).

361 Interestingly, these substantial differences in the implants' compositions and water uptake  
362 behaviors are "not fully" reflected in the observed release kinetics (Figure 5a). This is because  
363 drug release was almost complete within the first few days: the time period of implant  
364 formation. For instance, after 4 d only  $3.8 \pm 0.8$  and  $10.5 \pm 1.0$  % dexamethasone remained  
365 trapped within the implants based on Resomer RG 502H and Resomer RG 504H, respectively.  
366 These amounts were slowly released during the subsequent 3 weeks. The observed slower drug  
367 release from Resomer RG 504H-based implants compared to Resomer RG 502H-based  
368 implants can at least partially be attributed to the lower water contents of the systems (and, thus,  
369 denser polymer networks). Please note that with other drugs, which are not almost completely  
370 released within the first few days during implant formation, substantial differences in the



371 resulting release kinetics can be expected from Resomer RG 502H- and Resomer RG 504H-  
372 based implants, due to the fundamentally different conditions for drug release in these systems  
373 (Figures 5b and c).

374

### 375 **3.4. Impact of the polymer concentration**

376 Figure 6 shows the observed dexamethasone release kinetics from *in-situ* formed implants  
377 prepared with drug-polymer solutions in NMP containing 30 vs. 45% Resomer RG 502H, or  
378 15 vs. 30 % Resomer RG 504H. Please note that in the latter case, higher polymer  
379 concentrations lead to considerable viscosities, rendering injection difficult. The volume of the  
380 release medium was 2.25 mL, the initial drug content 0.25 %. As it can be seen, the polymer  
381 concentration in the liquid formulations affected the resulting drug release kinetics, irrespective  
382 of the PLGA polymer molecular weight: With increasing polymer concentration the  
383 dexamethasone release rate decreased. This can at least partially be attributed to differences in  
384 the implants' inner structure, as shown in Figure 7: At the top, cross-sections of freeze-dried  
385 implants based on Resomer RG 502H are illustrated, at the bottom cross-sections of implants  
386 based on Resomer RG 504H. The implants were lyophilized after 3 d exposure to phosphate  
387 buffer pH 7.4. Again, please note that caution should be paid because of potential artifact  
388 creation during freeze-drying. The dashed regions indicate the hollow central implant cavities.  
389 Clearly, higher polymer concentrations in the liquid formulations lead to smaller cavities. This  
390 can be attributed to the fact that PLGA precipitation started at the "liquid formulation – aqueous  
391 bulk fluid" interface. Subsequent PLGA precipitation "filled" the *in-situ* forming implants. In  
392 the case of higher polymer concentrations, more polymer was available to fill the interior of the  
393 systems, resulting in smaller cavities. The thicker the polymer shells, the longer are the  
394 diffusion pathways through the PLGA matrices to be overcome by the trapped drug. Thus,

395 higher polymer concentrations in the formulations lead to thicker polymer shells/barriers and,  
396 hence, slower drug release (irrespective of the polymer molecular weight).

397 Furthermore, the smaller central implant cavities at higher initial PLGA concentrations  
398 resulted in lower increases in the systems' wet mass and lower water contents, irrespective of  
399 the PLGA polymer molecular weight (Figures 8 and 9). Figures 10 to 12 illustrate the dynamic  
400 changes in the polymer molecular weight (Mw) of the PLGA, the pH of the surrounding bulk  
401 fluid and the dry mass loss kinetics of the systems. Importantly, the smaller central implant  
402 cavities observed at higher initial polymer concentrations lead to accelerated ester chain  
403 cleavage (Figure 10: open symbols always below filled symbols). This can be attributed to an  
404 increase in the importance of autocatalytic effects in these systems: Water is present throughout  
405 the implants, thus, polymer chain cleavage occurs in the entire polymer matrices. The generated  
406 (water-soluble) shorter chain acids slowly diffuse into the surrounding bulk fluid, where they  
407 are (at least partially) neutralized. In addition, bases from the surrounding phosphate buffer  
408 diffuse into the implants and neutralize (at least partially) the generated acids. However, the  
409 rate at which the acids are generated within the implants can be higher than the rate at which  
410 they are neutralized. Consequently, the micro-pH can locally drop (Brunner et al., 1999; Ding  
411 and Schwendeman, 2004; Li and Schwendeman, 2005; Ding and Schwendeman, 2008;  
412 Schädlich et al., 2014), resulting in pH gradients within the implants. Since hydrolytic ester  
413 bond cleavage is catalyzed by protons, PLGA degradation is accelerated at locations with low  
414 pH values (Grizzi et al., 1995; Lu et al., 1999). The importance of such autocatalytic effects  
415 strongly depends on the systems' dimensions and porosity (Siepmann et al., 2005; Klose et al.,  
416 2006). With increasing polymer concentration in the liquid formulation the thickness of the  
417 polymer "shells" increases (Figure 7), hence, autocatalysis is likely more pronounced. The  
418 experimentally measured PLGA degradation kinetics shown in Figure 10 clearly confirm this  
419 hypothesis: The polymer backbone is more rapidly cleaved at higher PLGA concentrations

420 (open vs. filled symbols). Interestingly, this faster PLGA degradation at higher polymer  
421 concentrations is not reflected in the drug release kinetics (Figure 6), demonstrating the  
422 dominance of the thickness of the PLGA shells (the lengths of the diffusion pathways through  
423 the polymeric matrices) in this case.

424 Furthermore, the diffusion of the short chain acids out of the implants into the surrounding  
425 bulk fluid can lead to a decrease in pH of the latter. As it can be seen in Figure 11, decreasing  
426 pH values of the release medium were indeed observed in all cases. At higher polymer  
427 concentrations the “pH drops” were much more pronounced than in the case of lower PLGA  
428 concentrations, irrespective of the polymer molecular weight. This can probably be attributed  
429 to the fact that thicker polymer “shells” are created at high PLGA concentrations, resulting in  
430 more pronounced autocatalytic effects (since the generated short chain acids more slowly  
431 diffuse out and bases from the release medium more slowly diffuse in, due to the longer  
432 diffusion pathways to be overcome). The potential consequences of (slight) acidifications of  
433 the surrounding environment in vivo should be addressed in future studies. The fact that  
434 dexamethasone is an anti-inflammatory drug might help minimizing tissue irritation, but  
435 caution should be taken when speculating on these aspects based on in vitro data.

436 Comparing the dynamic changes in the pH values of the surrounding bulk fluids in the case  
437 of implants based on Resomer RG 502H and Resomer RG 504H (Figure 11 a vs. 11b), it can  
438 be seen that the “pH drops” occur at later time points in the case of the longer chain PLGA.  
439 This can at least partially be attributed to the fact that the initial polymer molecular weight was  
440 higher, thus, more time is needed to generate short chain, water-soluble acids, which can diffuse  
441 out. Interestingly, the “*clear* pH drops” in the bulk fluid observed at higher polymer  
442 concentrations (open symbols in Figures 11a,b) are followed by distinct increases in the  
443 systems’ dry mass loss (open symbols in Figures 12a,b): The dry mass loss nicely reflects the  
444 leaching of the shorter chain (water-soluble) acids out of the implants into the release medium.

#### 445 **4. Conclusion**

446 *In-situ* forming PLGA-based implants offer an interesting potential for ocular  
447 dexamethasone delivery. Importantly, the systems can be expected to be rather robust with  
448 respect to variations in the vitreous humor volumes encountered *in vivo*. Depending on the  
449 initial drug loading, drug saturation effects *within* the implants and in the surrounding aqueous  
450 medium can play an important role for the control of dexamethasone release. The polymer  
451 molecular weight as well as the PLGA concentration in the liquid formulations determine *how*  
452 the macromolecules precipitate as well as the extent and rate of system swelling. These are key  
453 features, being decisive for the mobility of water, drug, polymer degradation products and bases  
454 within the system. For example, they affect the thickness of the polymer shell, water content of  
455 the system and importance of local drops in the micro-pH (and, thus, autocatalysis). The inner  
456 implant structure and conditions for mass transport within the *in-situ* forming implants  
457 determine polymer degradation and drug release.

458 In the future, the toxicity of the solvent NMP for the ocular tissue as well as the potential  
459 consequences of local drops in pH due to leaching of PLGA degradation products should be  
460 studied *in vivo*. It would also be interesting to investigate the effects of the monomer ratio  
461 (lactic acid to glycolic acid) of the PLGA as well as the impact of potential additives, altering  
462 the formation of the implants and the conditions for mass transport. Such formulation changes  
463 might be used to adjust desired release kinetics for given drugs and drug doses during specific  
464 target release periods.

465

466 **References**

- 467 Agossa, K., Lizambard, M., Rongthong, T., Delcourt-Debruyne, E., Siepmann, J., Siepmann,  
468 F., 2017. Physical key properties of antibiotic-free, PLGA/HPMC-based in-situ forming  
469 implants for local periodontitis treatment. *Int. J. Pharm.* 521, 282–293.  
470 <https://doi.org/10.1016/j.ijpharm.2017.02.039>
- 471 Bennett, L., 2016. Other Advances in Ocular Drug Delivery, in: Addo, R.T. (Ed.), *Ocular Drug*  
472 *Delivery: Advances, Challenges and Applications*. Springer International Publishing,  
473 pp. 165–185. [https://doi.org/10.1007/978-3-319-47691-9\\_10](https://doi.org/10.1007/978-3-319-47691-9_10)
- 474 Bisht, R., Jaiswal, J.K., Oliver, V.F., Eurtivong, C., Reynisson, J., Rupenthal, I.D., 2017.  
475 Preparation and evaluation of PLGA nanoparticle-loaded biodegradable light-  
476 responsive injectable implants as a promising platform for intravitreal drug delivery. *J.*  
477 *Drug Deliv. Sci. Technol.* 40, 142–156. <https://doi.org/10.1016/j.jddst.2017.06.006>
- 478 Bonilha, V.L., Shadrach, K.G., Rayborn, M.E., Li, Y., Pauer, G.J.T., Hagstrom, S.A.,  
479 Bhattacharya, S.K., Hollyfield, J.G., 2013. Retinal deimination and PAD2 levels in  
480 retinas from donors with age-related macular degeneration (AMD). *Exp. Eye Res.* 111,  
481 71–78. <https://doi.org/10.1016/j.exer.2013.03.017>
- 482 Brunner, A., Mäder, K., Göpferich, A., 1999. pH and Osmotic Pressure Inside Biodegradable  
483 Microspheres During Erosion1. *Pharm. Res.* 16, 847–853.  
484 <https://doi.org/10.1023/A:1018822002353>
- 485 Chan, A., Leung, L.-S., Blumenkranz, M.S., 2011. Critical appraisal of the clinical utility of the  
486 dexamethasone intravitreal implant (Ozurdex®) for the treatment of macular edema  
487 related to branch retinal vein occlusion or central retinal vein occlusion. *Clin.*  
488 *Ophthalmol. Auckl. NZ* 5, 1043–1049. <https://doi.org/10.2147/OPHTH.S13775>
- 489 Chiou, G.C.Y., 2011. Pharmacological treatment of dry age-related macular degeneration  
490 (AMD). *Taiwan J. Ophthalmol.* 1, 2–5. <https://doi.org/10.1016/j.tjo.2011.08.001>

- 491 Desai, K.G.H., Mallery, S.R., Schwendeman, S.P., 2008. Effect of formulation parameters on  
492 2-methoxyestradiol release from injectable cylindrical poly(dl-lactide-co-glycolide)  
493 implants. *Eur. J. Pharm. Biopharm.* 70, 187–198.  
494 <https://doi.org/10.1016/j.ejpb.2008.03.007>
- 495 Ding, A.G., Schwendeman, S.P., 2008. Acidic Microclimate pH Distribution in PLGA  
496 Microspheres Monitored by Confocal Laser Scanning Microscopy. *Pharm. Res.* 25,  
497 2041–2052. <https://doi.org/10.1007/s11095-008-9594-3>
- 498 Ding, A.G., Schwendeman, S.P., 2004. Determination of water-soluble acid distribution in  
499 poly(lactide-co-glycolide). *J. Pharm. Sci.* 93, 322–331.  
500 <https://doi.org/10.1002/jps.10524>
- 501 Do, M.P., Neut, C., Delcourt, E., Seixas Certo, T., Siepmann, J., Siepmann, F., 2014. In situ  
502 forming implants for periodontitis treatment with improved adhesive properties. *Eur. J.*  
503 *Pharm. Biopharm.* 88, 342–350. <https://doi.org/10.1016/j.ejpb.2014.05.006>
- 504 Do, M.P., Neut, C., Metz, H., Delcourt, E., Mäder, K., Siepmann, J., Siepmann, F., 2015a. In-  
505 situ forming composite implants for periodontitis treatment: How the formulation  
506 determines system performance. *Int. J. Pharm.* 486, 38–51.  
507 <https://doi.org/10.1016/j.ijpharm.2015.03.026>
- 508 Do, M.P., Neut, C., Metz, H., Delcourt, E., Siepmann, J., Mäder, K., Siepmann, F., 2015b.  
509 Mechanistic analysis of PLGA/HPMC-based in-situ forming implants for periodontitis  
510 treatment. *Eur. J. Pharm. Biopharm.* 94, 273–283.  
511 <https://doi.org/10.1016/j.ejpb.2015.05.018>
- 512 Droege, K.M., Muether, P.S., Hermann, M.M., Caramoy, A., Viebahn, U., Kirchhof, B., Fauser,  
513 S., 2013. Adherence to ranibizumab treatment for neovascular age-related macular  
514 degeneration in real life. *Graefes Arch. Clin. Exp. Ophthalmol.* 251, 1281–1284.  
515 <https://doi.org/10.1007/s00417-012-2177-3>

- 516 Edelhauser, H.F., Rowe-Rendleman, C.L., Robinson, M.R., Dawson, D.G., Chader, G.J.,  
517 Grossniklaus, H.E., Rittenhouse, K.D., Wilson, C.G., Weber, D.A., Kuppermann, B.D.,  
518 Csaky, K.G., Olsen, T.W., Kompella, U.B., Holers, V.M., Hageman, G.S., Gilger, B.C.,  
519 Campochiaro, P.A., Whitcup, S.M., Wong, W.T., 2010. Ophthalmic Drug Delivery  
520 Systems for the Treatment of Retinal Diseases: Basic Research to Clinical Applications.  
521 *Investig. Ophthalmology Vis. Sci.* 51, 5403. <https://doi.org/10.1167/iovs.10-5392>
- 522 Fredenberg, S., Wahlgren, M., Reslow, M., Axelsson, A., 2011. The mechanisms of drug  
523 release in poly(lactic-co-glycolic acid)-based drug delivery systems—A review. *Int. J.*  
524 *Pharm.* 415, 34–52. <https://doi.org/10.1016/j.ijpharm.2011.05.049>
- 525 Gasmi, H., Danede, F., Siepmann, J., Siepmann, F., 2015a. Does PLGA microparticle swelling  
526 control drug release? New insight based on single particle swelling studies. *J. Controlled*  
527 *Release* 213, 120–127. <https://doi.org/10.1016/j.jconrel.2015.06.039>
- 528 Gasmi, H., Siepmann, F., Hamoudi, M.C., Danede, F., Verin, J., Willart, J.-F., Siepmann, J.,  
529 2016. Towards a better understanding of the different release phases from PLGA  
530 microparticles: Dexamethasone-loaded systems. *Int. J. Pharm.*, In Honour of Professor  
531 Alexander T. Florence In Honour of Professor Alexander T. Florence 514, 189–199.  
532 <https://doi.org/10.1016/j.ijpharm.2016.08.032>
- 533 Gasmi, H., Willart, J.-F., Danede, F., Hamoudi, M.C., Siepmann, J., Siepmann, F., 2015b.  
534 Importance of PLGA microparticle swelling for the control of prilocaine release. *J. Drug*  
535 *Deliv. Sci. Technol.* 30, 123–132. <https://doi.org/10.1016/j.jddst.2015.10.009>
- 536 Ghalanbor, Z., Körber, M., Bodmeier, R., 2013. Interdependency of protein-release  
537 completeness and polymer degradation in PLGA-based implants. *Eur. J. Pharm.*  
538 *Biopharm.* 85, 624–630. <https://doi.org/10.1016/j.ejpb.2013.03.031>

- 539 Ghazala, F., Hovan, M., Mahmood, S., 2013. Improving treatment provision of Wet AMD with  
540 intravitreal ranibizumab. *BMJ Qual. Improv. Rep.* 2, u201733.w993.  
541 <https://doi.org/10.1136/bmjquality.u201733.w993>
- 542 Giudice, G.L., Galan, A., 2012. Basic Research and Clinical Application of Drug Delivery  
543 Systems for the Treatment of Age-Related Macular Degeneration.  
544 <https://doi.org/10.5772/31524>
- 545 Grizzi, I., Garreau, H., Li, S., Vert, M., 1995. Hydrolytic degradation of devices based on  
546 poly(dl-lactic acid) size-dependence. *Biomaterials* 16, 305–311.  
547 [https://doi.org/10.1016/0142-9612\(95\)93258-F](https://doi.org/10.1016/0142-9612(95)93258-F)
- 548 Hamoudi-Ben Yelles, M.C., Tran Tan, V., Danede, F., Willart, J.F., Siepmann, J., 2017. PLGA  
549 implants: How Poloxamer/PEO addition slows down or accelerates polymer  
550 degradation and drug release. *J. Controlled Release* 253, 19–29.  
551 <https://doi.org/10.1016/j.jconrel.2017.03.009>
- 552 Hirota, K., Doty, A.C., Ackermann, R., Zhou, J., Olsen, K.F., Feng, M.R., Wang, Y., Choi, S.,  
553 Qu, W., Schwendeman, A.S., Schwendeman, S.P., 2016. Characterizing release  
554 mechanisms of leuprolide acetate-loaded PLGA microspheres for IVIVC development  
555 I: In vitro evaluation. *J. Controlled Release*, The 14th edition of the European  
556 Symposium on Controlled Drug Delivery, Egmond aan Zee, The Netherlands on April  
557 13-15, 2016 244, 302–313. <https://doi.org/10.1016/j.jconrel.2016.08.023>
- 558 Huang, J., Mazzara, J.M., Schwendeman, S.P., Thouless, M.D., 2015. Self-healing of pores in  
559 PLGAs. *J. Controlled Release* 206, 20–29.  
560 <https://doi.org/10.1016/j.jconrel.2015.02.025>
- 561 Hughes, P.M., Olejnik, O., Chang-Lin, J.-E., Wilson, C.G., 2005. Topical and systemic drug  
562 delivery to the posterior segments. *Adv. Drug Deliv. Rev.*, Drug Delivery Strategies to



- 563 Treat Age-Related Macular Degeneration 57, 2010–2032.  
564 <https://doi.org/10.1016/j.addr.2005.09.004>
- 565 Kaur, I.P., Kakkar, S., 2014. Nanotherapy for posterior eye diseases. *J. Controlled Release* 193,  
566 100–112. <https://doi.org/10.1016/j.jconrel.2014.05.031>
- 567 Kempe, S., Mäder, K., 2012. In situ forming implants — an attractive formulation principle for  
568 parenteral depot formulations. *J. Controlled Release, Drug Delivery Research in Europe*  
569 161, 668–679. <https://doi.org/10.1016/j.jconrel.2012.04.016>
- 570 Kempe, S., Metz, H., Pereira, P.G.C., Mäder, K., 2010. Non-invasive in vivo evaluation of in  
571 situ forming PLGA implants by benchtop magnetic resonance imaging (BT-MRI) and  
572 EPR spectroscopy. *Eur. J. Pharm. Biopharm., Imaging Techniques in Drug*  
573 *Development* 74, 102–108. <https://doi.org/10.1016/j.ejpb.2009.06.008>
- 574 Klose, D., Siepmann, F., Elkharraz, K., Krenzlin, S., Siepmann, J., 2006. How porosity and size  
575 affect the drug release mechanisms from PLGA-based microparticles. *Int. J. Pharm.,*  
576 *Local Controlled Drug Delivery to the Brain* 314, 198–206.  
577 <https://doi.org/10.1016/j.ijpharm.2005.07.031>
- 578 Kowluru, R.A., Mishra, M., 2015. Oxidative stress, mitochondrial damage and diabetic  
579 retinopathy. *Biochim. Biophys. Acta BBA - Mol. Basis Dis.* 1852, 2474–2483.  
580 <https://doi.org/10.1016/j.bbadis.2015.08.001>
- 581 Kranz, H., Bodmeier, R., 2008. Structure formation and characterization of injectable drug  
582 loaded biodegradable devices: In situ implants versus in situ microparticles. *Eur. J.*  
583 *Pharm. Sci.* 34, 164–172. <https://doi.org/10.1016/j.ejps.2008.03.004>
- 584 Kranz, H., Bodmeier, R., 2007. A novel in situ forming drug delivery system for controlled  
585 parenteral drug delivery. *Int. J. Pharm.* 332, 107–114.  
586 <https://doi.org/10.1016/j.ijpharm.2006.09.033>

- 587 Kranz, H., Ubrich, N., Maincent, P., Bodmeier, R., 2000. Physicomechanical Properties of  
588 Biodegradable Poly(D,L-lactide) and Poly(D,L-lactide-co-glycolide) Films in the Dry  
589 and Wet States. *J. Pharm. Sci.* 89, 1558–1566. [https://doi.org/10.1002/1520-  
590 6017\(200012\)89:12<1558::AID-JPS6>3.0.CO;2-8](https://doi.org/10.1002/1520-6017(200012)89:12<1558::AID-JPS6>3.0.CO;2-8)
- 591 Kurz, P.A., Suhler, E.B., Flaxel, C.J., Rosenbaum, J.T., 2008. Injectable Intraocular  
592 Corticosteroids, in: Becker, M., Davis, J. (Eds.), *Surgical Management of Inflammatory  
593 Eye Disease*. Springer Berlin Heidelberg, pp. 5–16. [https://doi.org/10.1007/978-3-540-  
594 33862-8\\_1](https://doi.org/10.1007/978-3-540-33862-8_1)
- 595 Li, L., Schwendeman, S.P., 2005. Mapping neutral microclimate pH in PLGA microspheres. *J.  
596 Controlled Release, Proceedings of the Eight European Symposium on Controlled Drug  
597 Delivery* 101, 163–173. <https://doi.org/10.1016/j.jconrel.2004.07.029>
- 598 Lu, L., Garcia, C.A., Mikos, A.G., 1999. In vitro degradation of thin poly(DL-lactic-co-glycolic  
599 acid) films. *J. Biomed. Mater. Res.* 46, 236–244.
- 600 Luan, X., Skupin, M., Siepmann, J., Bodmeier, R., 2006. Key parameters affecting the initial  
601 release (burst) and encapsulation efficiency of peptide-containing poly(lactide-co-  
602 glycolide) microparticles. *Int. J. Pharm.* 324, 168–175.  
603 <https://doi.org/10.1016/j.ijpharm.2006.06.004>
- 604 Parent, M., Clarot, I., Gibot, S., Derive, M., Maincent, P., Leroy, P., Boudier, A., 2017. One-  
605 week in vivo sustained release of a peptide formulated into in situ forming implants. *Int.  
606 J. Pharm.* 521, 357–360. <https://doi.org/10.1016/j.ijpharm.2017.02.046>
- 607 Parent, M., Nouvel, C., Koerber, M., Sapin, A., Maincent, P., Boudier, A., 2013. PLGA in situ  
608 implants formed by phase inversion: Critical physicochemical parameters to modulate  
609 drug release. *J. Controlled Release* 172, 292–304.  
610 <https://doi.org/10.1016/j.jconrel.2013.08.024>

- 611 Rodrigues, E.B., Grumann, A., Penha, F.M., Shiroma, H., Rossi, E., Meyer, C.H., Stefano, V.,  
612 Maia, M., Magalhaes, O., Farah, M.E., 2011. Effect of needle type and injection  
613 technique on pain level and vitreal reflux in intravitreal injection. *J. Ocul. Pharmacol.*  
614 *Ther. Off. J. Assoc. Ocul. Pharmacol. Ther.* 27, 197–203.  
615 <https://doi.org/10.1089/jop.2010.0082>
- 616 Rodríguez Villanueva, J., Rodríguez Villanueva, L., Guzmán Navarro, M., 2017.  
617 Pharmaceutical technology can turn a traditional drug, dexamethasone into a first-line  
618 ocular medicine. A global perspective and future trends. *Int. J. Pharm.* 516, 342–351.  
619 <https://doi.org/10.1016/j.ijpharm.2016.11.053>
- 620 Schädlich, A., Kempe, S., Mäder, K., 2014. Non-invasive in vivo characterization of  
621 microclimate pH inside in situ forming PLGA implants using multispectral fluorescence  
622 imaging. *J. Controlled Release* 179, 52–62.  
623 <https://doi.org/10.1016/j.jconrel.2014.01.024>
- 624 Schoenhammer, K., Boisclair, J., Schuetz, H., Petersen, H., Goepferich, A., 2010.  
625 Biocompatibility of an injectable in situ forming depot for peptide delivery. *J. Pharm.*  
626 *Sci.* 99, 4390–4399. <https://doi.org/10.1002/jps.22149>
- 627 Schoenhammer, K., Petersen, H., Guethlein, F., Goepferich, A., 2009. Injectable in situ forming  
628 depot systems: PEG-DAE as novel solvent for improved PLGA storage stability. *Int. J.*  
629 *Pharm.* 371, 33–39. <https://doi.org/10.1016/j.ijpharm.2008.12.019>
- 630 Schwendeman, S.P., Shah, R.B., Bailey, B.A., Schwendeman, A.S., 2014. Injectable controlled  
631 release depots for large molecules. *J. Controlled Release*, 30th Anniversary Special  
632 Issue 190, 240–253. <https://doi.org/10.1016/j.jconrel.2014.05.057>
- 633 Siepman, J., Elkharraz, K., Siepman, F., Klose, D., 2005. How Autocatalysis Accelerates  
634 Drug Release from PLGA-Based Microparticles: A Quantitative Treatment.  
635 *Biomacromolecules* 6, 2312–2319. <https://doi.org/10.1021/bm050228k>

- 636 Siepmann, J., Siepmann, F., 2012. Modeling of diffusion controlled drug delivery. *J. Controlled*  
637 *Release, Drug Delivery Research in Europe* 161, 351–362.  
638 <https://doi.org/10.1016/j.jconrel.2011.10.006>
- 639 Siepmann, J., Siepmann, F., 2008. Mathematical modeling of drug delivery. *Int. J. Pharm.,*  
640 *Future Perspectives in Pharmaceutics Contributions from Younger Scientists* 364, 328–  
641 343. <https://doi.org/10.1016/j.ijpharm.2008.09.004>
- 642 Thakur, R.R.S., McMillan, H.L., Jones, D.S., 2014. Solvent induced phase inversion-based in  
643 situ forming controlled release drug delivery implants. *J. Controlled Release* 176, 8–23.  
644 <https://doi.org/10.1016/j.jconrel.2013.12.020>
- 645 Toris, C.B., Yablonski, M.E., Wang, Y.-L., Camras, C.B., 1999. Aqueous humor dynamics in  
646 the aging human eye. *Am. J. Ophthalmol.* 127, 407–412. [https://doi.org/10.1016/S0002-](https://doi.org/10.1016/S0002-9394(98)00436-X)  
647 [9394\(98\)00436-X](https://doi.org/10.1016/S0002-9394(98)00436-X)
- 648 Ueda, H., Hacker, M. c., Haesslein, A., Jo, S., Ammon, D. m., Borazjani, R. n., Kunzler, J. f.,  
649 Salamone, J. c., Mikos, A. g., 2007. Injectable, in situ forming poly(propylene  
650 fumarate)-based ocular drug delivery systems. *J. Biomed. Mater. Res. A* 83A, 656–666.  
651 <https://doi.org/10.1002/jbm.a.31226>
- 652 Urtti, A., 2006. Challenges and obstacles of ocular pharmacokinetics and drug delivery. *Adv.*  
653 *Drug Deliv. Rev., Ocular Drug Delivery* 58, 1131–1135.  
654 <https://doi.org/10.1016/j.addr.2006.07.027>
- 655 Wan, T.-T., Li, X.-F., Sun, Y.-M., Li, Y.-B., Su, Y., 2015. Recent advances in understanding  
656 the biochemical and molecular mechanism of diabetic retinopathy. *Biomed.*  
657 *Pharmacother.* 74, 145–147. <https://doi.org/10.1016/j.biopha.2015.08.002>
- 658 Wilson, C.G., Tan, L.E., Mains, J., 2011. Principles of Retinal Drug Delivery from Within the  
659 Vitreous, in: Kompella, U.B., Edelhauser, H.F. (Eds.), *Drug Product Development for*

660 the Back of the Eye, AAPS Advances in the Pharmaceutical Sciences Series. Springer  
661 US, pp. 125–158.

662 Wykoff, C.C., Croft, D.E., Brown, D.M., Wang, R., Payne, J.F., Clark, L., Abdelfattah, N.S.,  
663 Sadda, S.R., 2015. Prospective Trial of Treat-and-Extend versus Monthly Dosing for  
664 Neovascular Age-Related Macular Degeneration: TREX-AMD 1-Year Results.  
665 Ophthalmology 122, 2514–2522. <https://doi.org/10.1016/j.ophtha.2015.08.009>

666 Yasin, M.N., Svirskis, D., Seyfoddin, A., Rupenthal, I.D., 2014. Implants for drug delivery to  
667 the posterior segment of the eye: A focus on stimuli-responsive and tunable release  
668 systems. J. Controlled Release 196, 208–221.  
669 <https://doi.org/10.1016/j.jconrel.2014.09.030>

670 Ying, L., Tahara, K., Takeuchi, H., 2013. Drug delivery to the ocular posterior segment using  
671 lipid emulsion via eye drop administration: Effect of emulsion formulations and surface  
672 modification. Int. J. Pharm. 453, 329–335.  
673 <https://doi.org/10.1016/j.ijpharm.2013.06.024>

674 Zaki, W.M.D.W., Zulkifley, M.A., Hussain, A., Halim, W.H.W.A., Mustafa, N.B.A., Ting,  
675 L.S., 2016. Diabetic retinopathy assessment: Towards an automated system. Biomed.  
676 Signal Process. Control 24, 72–82. <https://doi.org/10.1016/j.bspc.2015.09.011>

677

#### 678 **Web references**

679 <http://eligard.com>, accessed on 30 June 2018

680 <https://iluvien.com>, accessed on January 30 2018

681 <https://www.merck-animal-health-usa.com/product/cattle/Nuflor-Injectable-Solution/1>,  
682 accessed on 30 June 2018

683 <http://www.retisert.com>, accessed on January 30 2018

684 <https://www.zoetisus.com/products/dogs/doxirobe-gel.aspx>, accessed on 30 June 2018

**Figure legends**

686

687 Fig. 1. Macroscopic pictures of implants formed *in-situ* upon exposure to phosphate buffer  
688 pH 7.4 before and after freeze drying (surfaces and cross-sections). The formulations  
689 contained 0.75 % dexamethasone and 30 % PLGA 502H. The volume of the release  
690 medium was 2.25 mL (left column) or 4.5 mL (right column). The pictures were taken  
691 after 3 d. The dashed regions highlight the hollow cores of the implants.

692 Fig 2. Impact of the volume of the release medium (phosphate buffer pH 7.4) on: a) drug  
693 release, and b) the dynamic changes in the water/NMP content of *in-situ* forming  
694 implants. The formulations contained 0.75 % dexamethasone and 30 % PLGA 502H.  
695 Mean values +/- standard deviation are indicated (n=3).

696 Fig. 3. Impact of the initial drug loading (indicated in the diagrams) of *in-situ* forming  
697 implants on the resulting: a) drug release kinetics, b) dynamic changes in the wet mass  
698 and c) dynamic changes in the water/NMP content of the systems after exposure to  
699 phosphate buffer pH 7.4. The formulations contained 30 % PLGA 502H. The volume  
700 of the release medium was 2.25 mL. Mean values +/- standard deviation are indicated  
701 (n=3).

702 Fig. 4. Impact of the sampling frequency during the drug release measurements on: a) the  
703 cumulative relative amount of drug released, and b) the degree of saturation of the  
704 withdrawn samples. The formulations contained 7.5 % dexamethasone and 30 %  
705 PLGA 502H. The volume of the release medium was 4.5 mL. Mean values +/-  
706 standard deviation are indicated (n=3).

707 Fig. 5. Importance of the polymer molecular weight of the PLGA (Resomer 502H vs. 504H)  
708 for: a) drug release, b) the dynamic changes in the wet mass, and c) the dynamic  
709 changes in the water/NMP content from/of implants formed *in-situ* upon exposure to  
710 phosphate buffer pH 7.4. The formulations contained 0.25 % dexamethasone and

711 30 % PLGA. The volume of the release medium was 2.25 mL. Mean values +/-  
712 standard deviation are indicated (n=3).

713 Fig. 6. Impact of the PLGA concentration in the formulation on the resulting dexamethasone  
714 release kinetics from *in-situ* formed implants upon exposure to 2.25 mL phosphate  
715 buffer pH 7.4: a) PLGA 502H and b) PLGA 504H. The drug content was 0.25 %.  
716 Mean values +/- standard deviation are indicated (n=3).

717 Fig. 7. Macroscopic pictures of cross-sections of freeze-dried *in-situ* formed implants after  
718 3 d exposure to 2.25 mL phosphate buffer 7.4. The formulations contained 0.25 %  
719 dexamethasone and 30 % or 45 % PLGA 502H or 15 % or 30 % PLGA 504H. The  
720 cross-sections were obtained by manual breaking. All implants were hollow, the  
721 cavities are highlighted by the dashed areas.

722 Fig. 8. Impact of the PLGA concentration in the formulation on the dynamic changes in the  
723 wet mass of implants formed *in-situ* upon exposure to 2.25 mL phosphate buffer  
724 pH 7.4: a) PLGA 502H and b) PLGA 504H. The formulations contained 0.25 %  
725 dexamethasone. Mean values +/- standard deviation are indicated (n=3).

726 Fig. 9. Effects of the PLGA concentration in the formulation on the dynamic changes in the  
727 water/NMP content of implants formed *in-situ* upon exposure to 2.25 mL phosphate  
728 buffer pH 7.4: a) PLGA 502H and b) PLGA 504H. The formulations contained  
729 0.25 % dexamethasone. Mean values +/- standard deviation are indicated (n=3).

730 Fig. 10. Impact of the PLGA concentration in the formulation on PLGA degradation in  
731 implants formed *in-situ* upon exposure to 2.25 mL phosphate buffer pH 7.4: a) PLGA  
732 502H and b) PLGA 504H. The formulations contained 0.25 % dexamethasone. Mean  
733 values +/- standard deviation are indicated (n=3).

734 Fig. 11. Effects of the PLGA concentration in the formulation on the dynamic changes in the  
735 pH of the release medium surrounding implants formed *in-situ* upon exposure to

736 2.25 mL phosphate buffer pH 7.4: a) PLGA 502H and b) PLGA 504H. The  
737 formulations contained 0.25 % dexamethasone. Mean values +/- standard deviation  
738 are indicated (n=3).

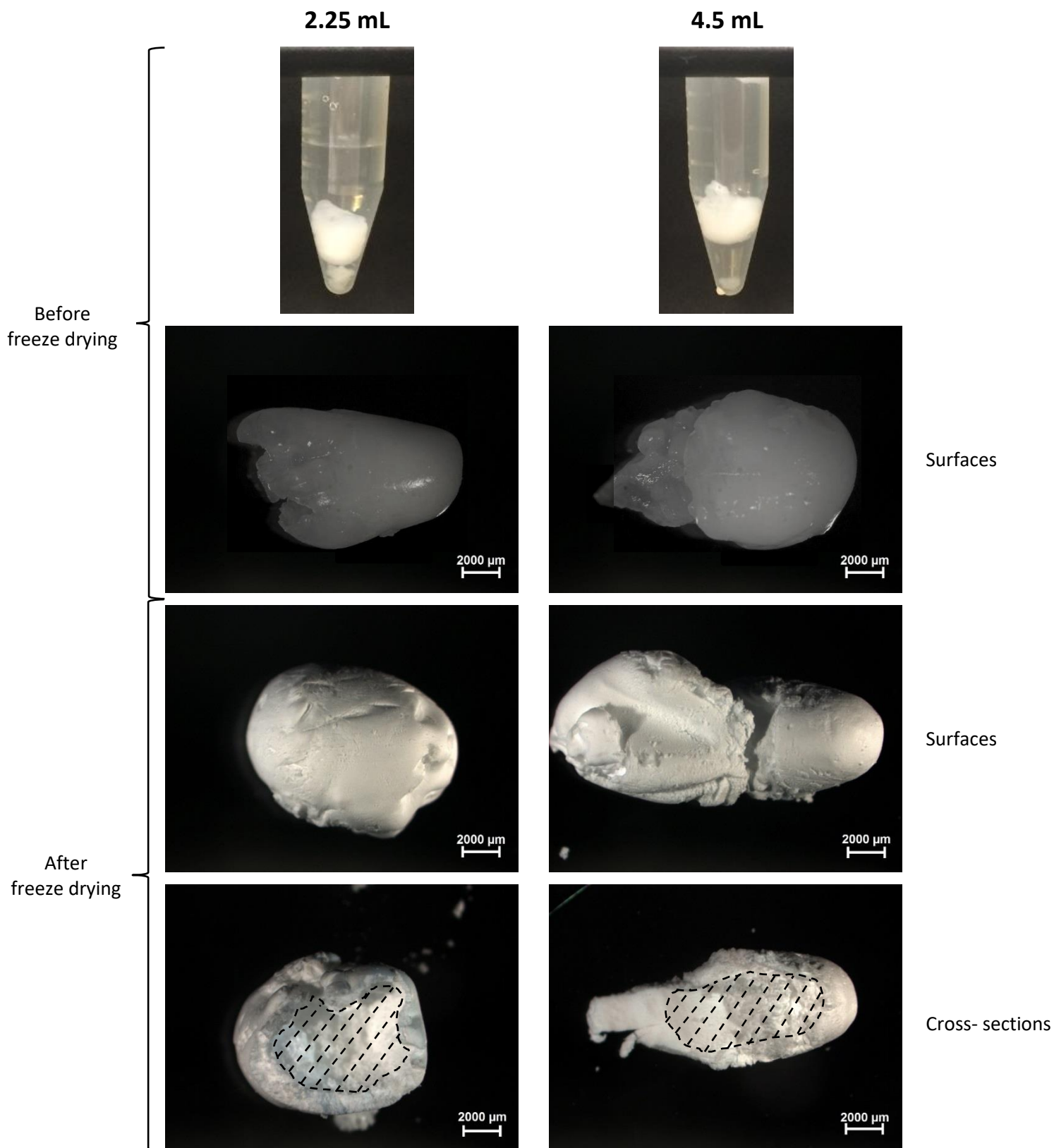
739 Fig. 12. Impact of the PLGA concentration in the formulation on the dry mass loss of implants  
740 formed *in-situ* upon exposure to 2.25 mL phosphate buffer pH 7.4: a) PLGA 502H  
741 and b) PLGA 504H. The formulations contained 0.25 % dexamethasone. Mean values  
742 +/- standard deviation are indicated (n=3).

743



744

745



746

747

Figure 1

748  
749  
750  
751  
752  
753  
754  
755  
756  
757  
758  
759  
760  
761  
762  
763  
764  
765  
766  
767  
768  
769  
770  
771  
772  
773  
774  
775  
776  
777  
778  
779

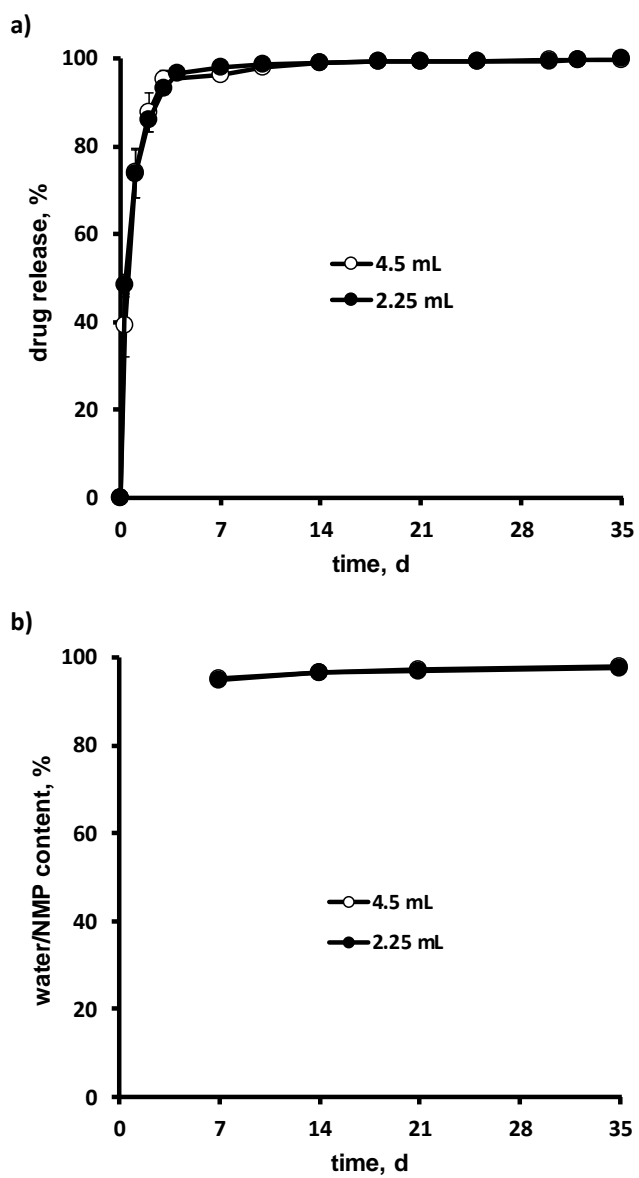


Figure 2

780  
781  
782  
783  
784  
785  
786  
787  
788  
789  
790  
791  
792  
793  
794  
795  
796  
797  
798  
799  
800  
801  
802  
803  
804  
805  
806  
807  
808  
809  
810  
811  
812  
813  
814  
815

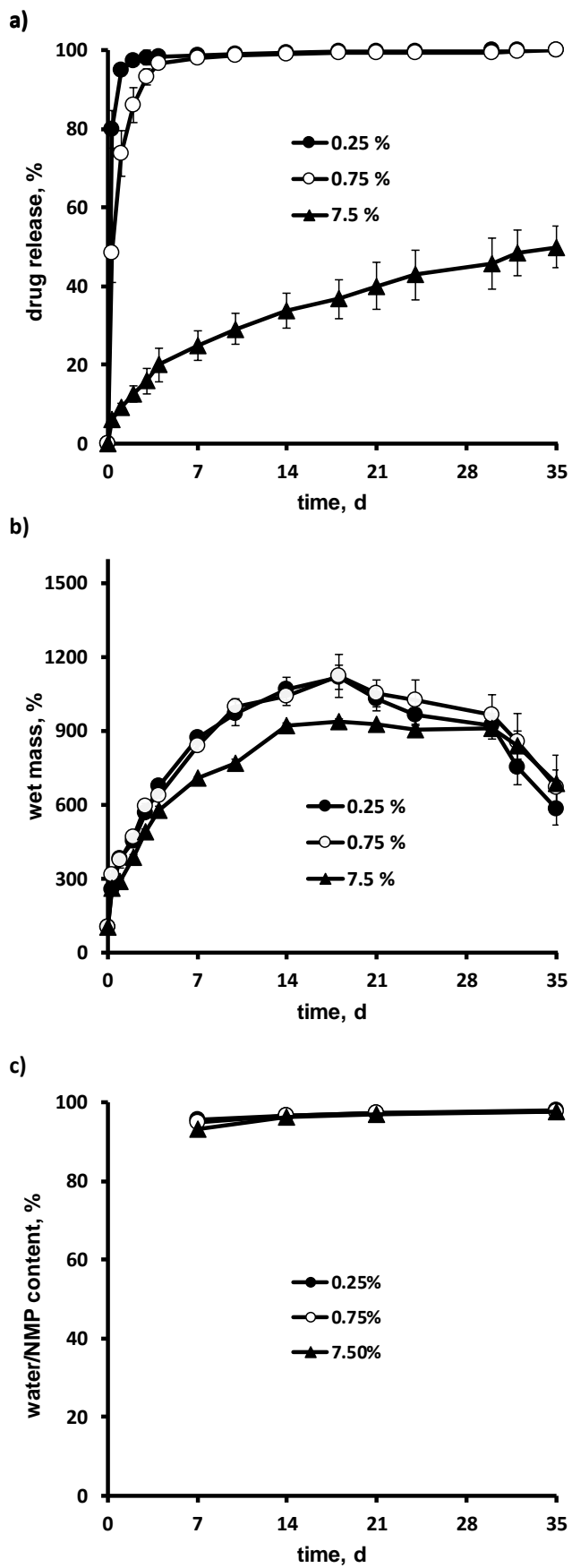


Figure 3

816  
817  
818  
819  
820  
821  
822  
823  
824  
825  
826  
827  
828  
829  
830  
831  
832  
833  
834  
835  
836  
837  
838  
839  
840  
841  
842  
843  
844  
845  
846  
847  
848

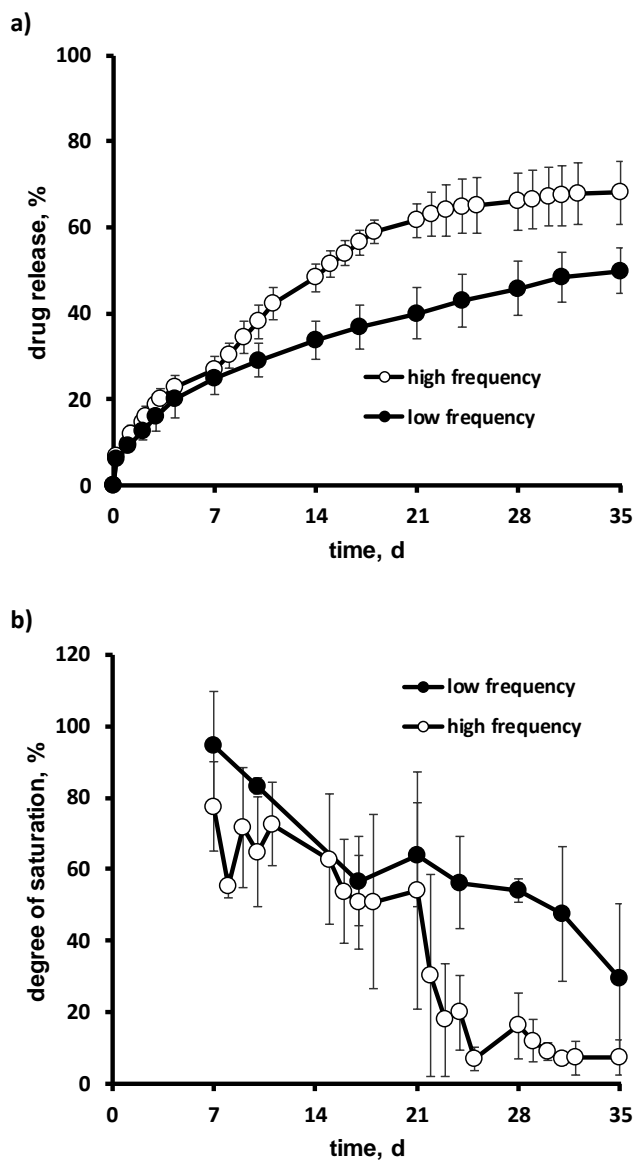


Figure 4

849  
850  
851  
852  
853  
854  
855  
856  
857  
858  
859  
860  
861  
862  
863  
864  
865  
866  
867  
868  
869  
870  
871  
872  
873  
874  
875  
876  
877  
878  
879  
880  
881  
882  
883  
884

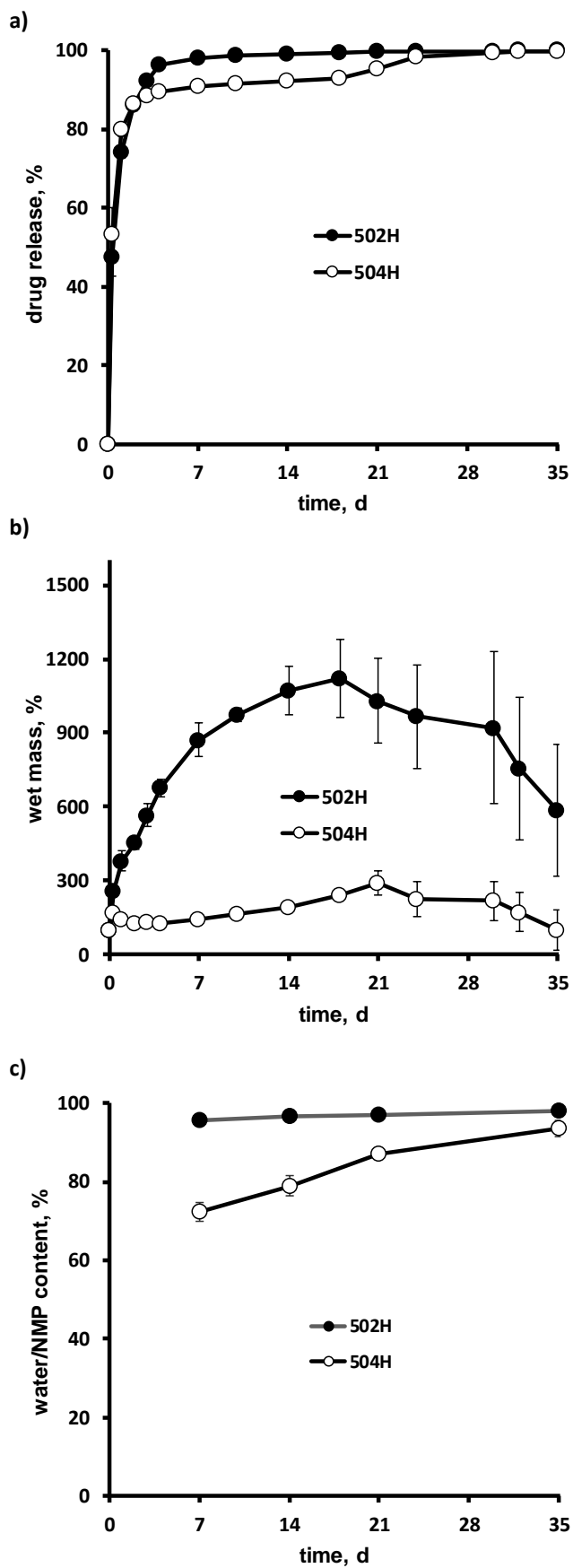


Figure 5

885  
886  
887  
888  
889  
890  
891  
892  
893  
894  
895  
896  
897  
898  
899  
900  
901  
902  
903  
904  
905  
906  
907  
908  
909  
910  
911  
912  
913  
914  
915  
916

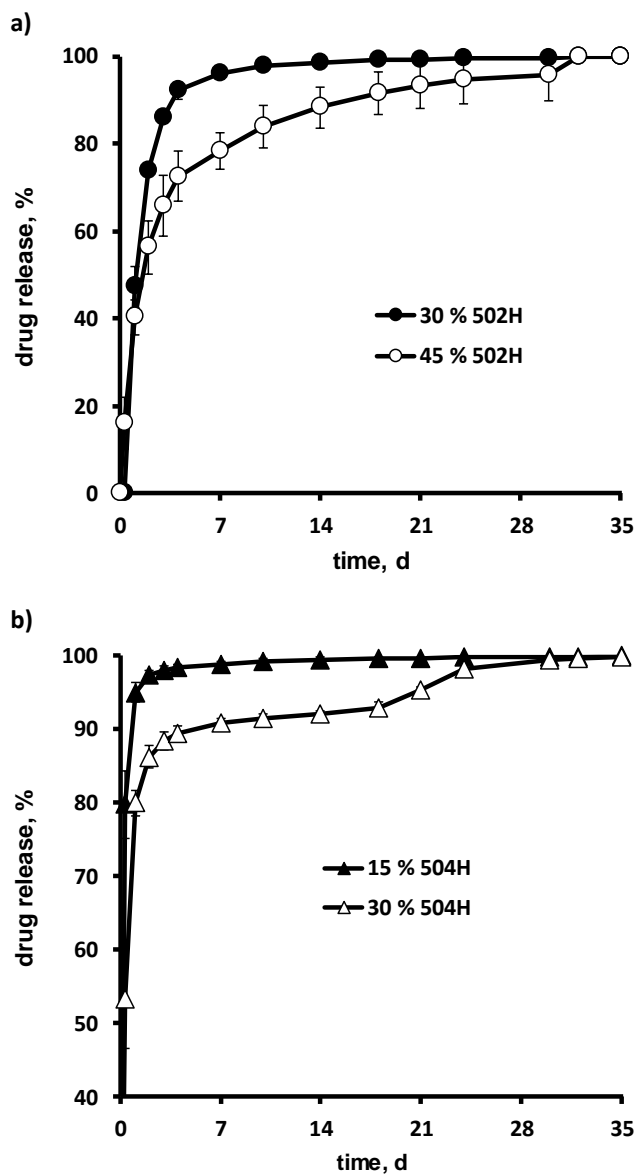
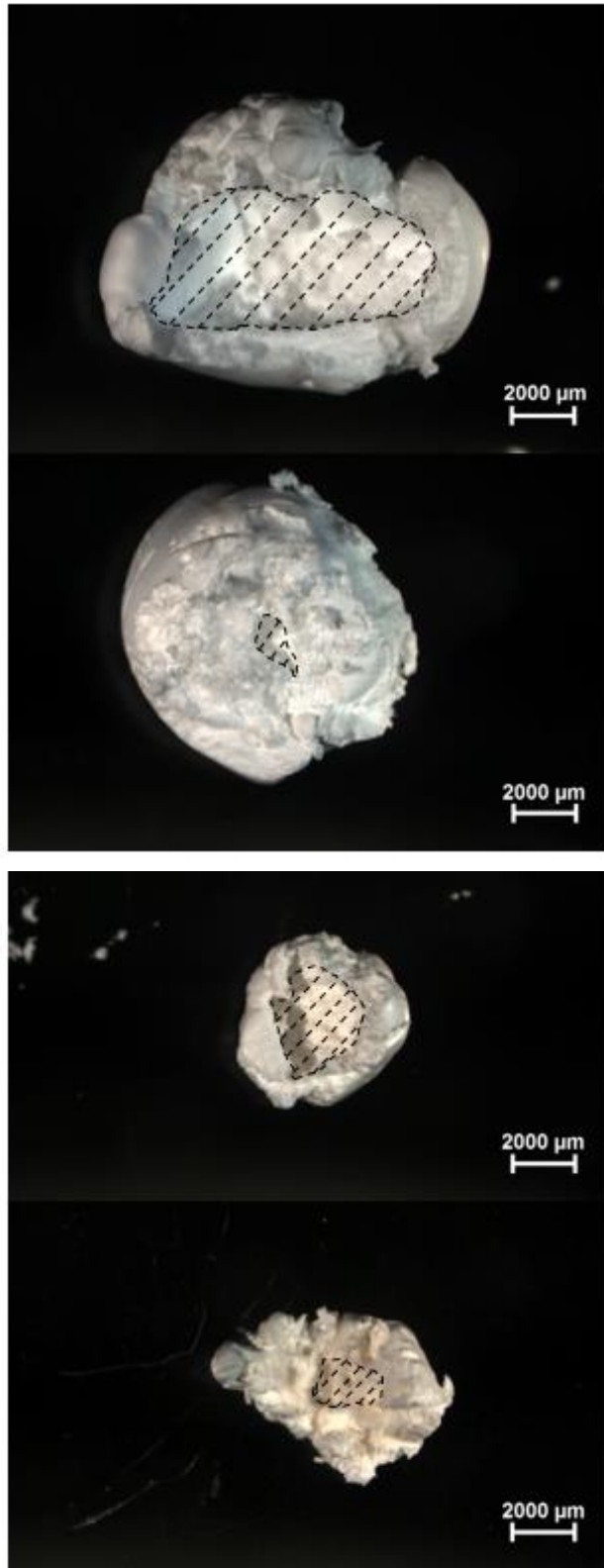


Figure 6



30 % 502H

45 % 502H

15 % 504H

30 % 504H

917

918

919

Figure 7

920  
921  
922  
923  
924  
925  
926  
927  
928  
929  
930  
931  
932  
933  
934  
935  
936  
937  
938  
939  
940  
941  
942  
943  
944  
945  
946  
947  
948  
949  
950  
951  
952  
953  
954  
955

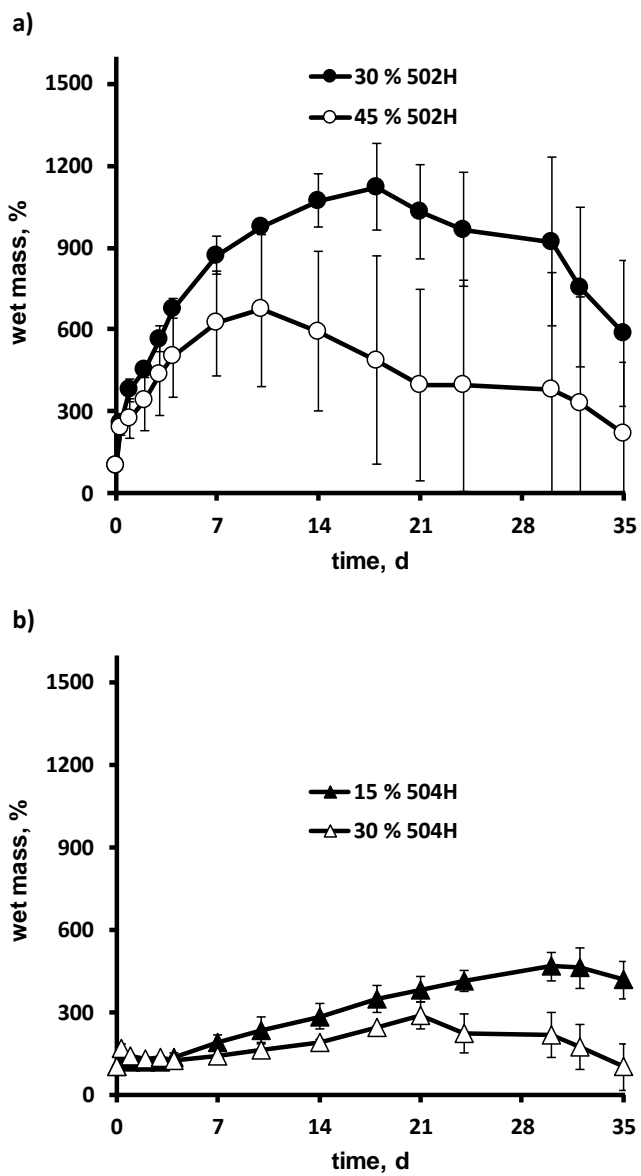


Figure 8



956  
957  
958  
959  
960  
961  
962  
963  
964  
965  
966  
967  
968  
969  
970  
971  
972  
973  
974  
975  
976  
977  
978  
979  
980  
981  
982  
983  
984  
985  
986  
987  
988  
989

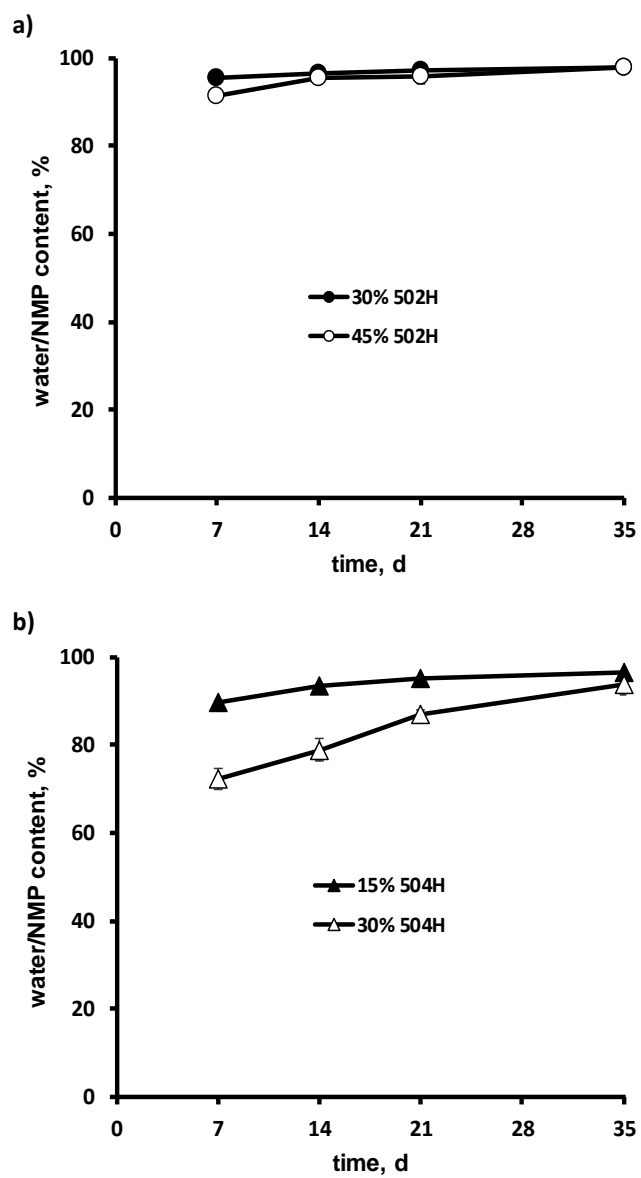


Figure 9

990  
991  
992  
993  
994  
995  
996  
997  
998  
999  
1000  
1001  
1002  
1003  
1004  
1005  
1006  
1007  
1008  
1009  
1010  
1011  
1012  
1013  
1014  
1015  
1016  
1017  
1018  
1019  
1020  
1021

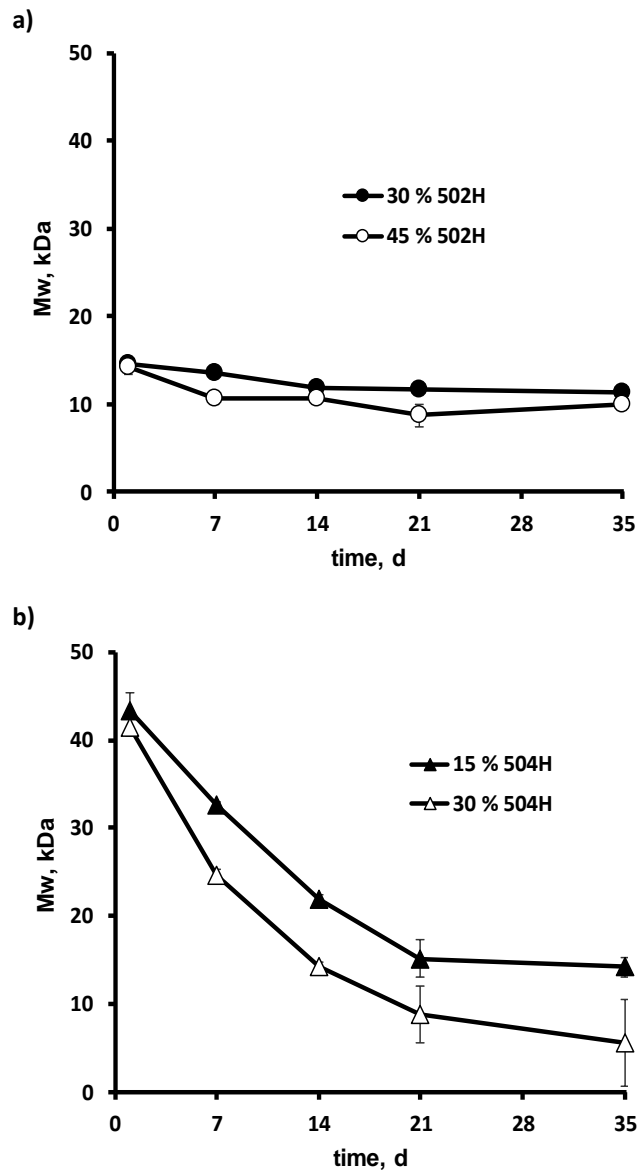


Figure 10

1022  
1023  
1024  
1025  
1026  
1027  
1028  
1029  
1030  
1031  
1032  
1033  
1034  
1035  
1036  
1037  
1038  
1039  
1040  
1041  
1042  
1043  
1044  
1045  
1046  
1047  
1048  
1049  
1050  
1051  
1052  
1053  
1054  
1055

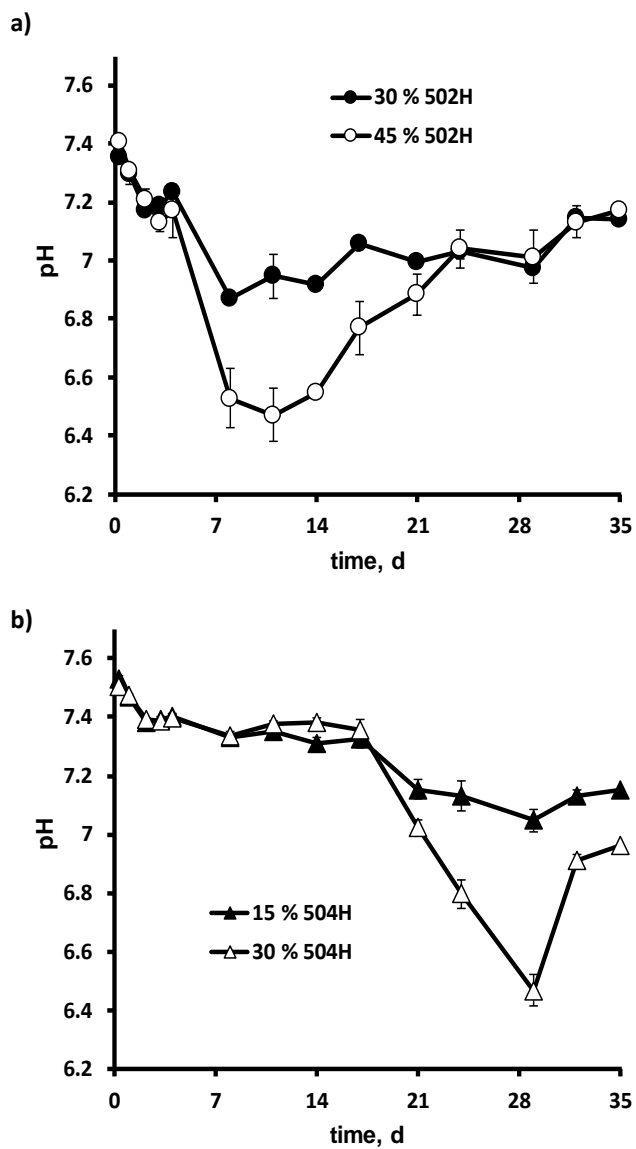


Figure 11

1056  
1057  
1058  
1059  
1060  
1061  
1062  
1063  
1064  
1065  
1066  
1067  
1068  
1069  
1070  
1071  
1072  
1073  
1074  
1075  
1076  
1077  
1078  
1079  
1080  
1081  
1082  
1083  
1084  
1085  
1086  
1087

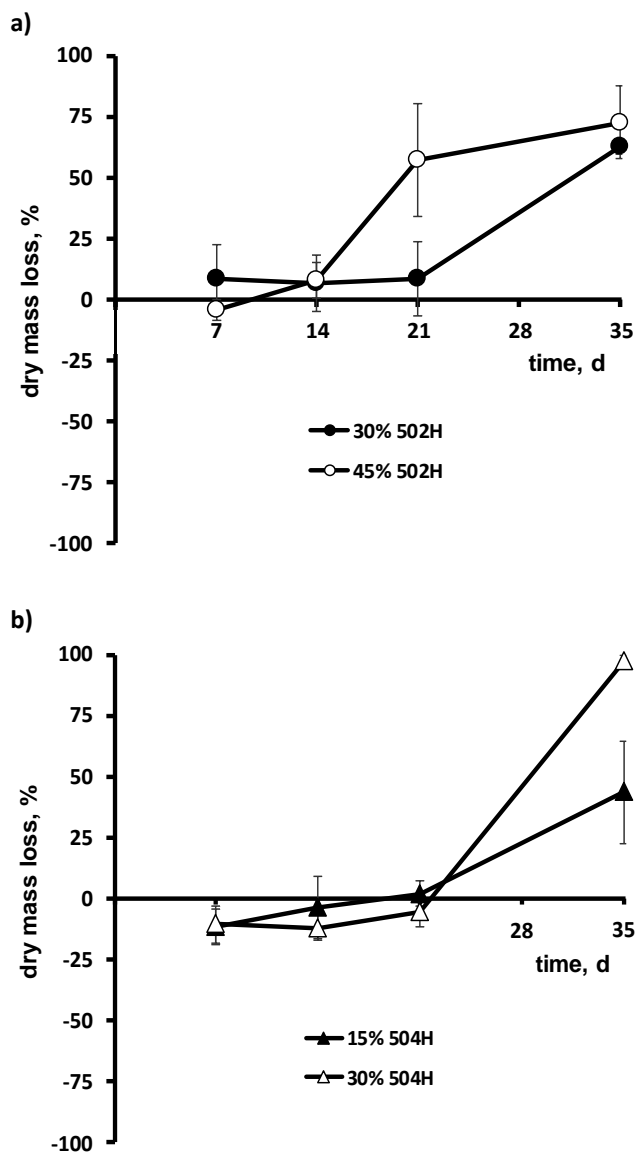


Figure 12